Journal of Chromatography A, 1217 (2010) 2022–2031

Contents lists available at ScienceDirect

Journal of Chromatography A

journal homepage: www.elsevier.com/locate/chroma

Towards a solution for viscous heating in ultra-high pressure liquid chromatography using intermediate cooling

K. Broeckhoven[a], J. Billen[a], M. Verstraeten[a], K. Choikhet[b], M. Dittmann[b], G. Rozing[b], G. Desmet[a,*]

[a] Vrije Universiteit Brussel, Department of Chemical Engineering (CHIS-IR), Pleinlaan 2, 1050 Brussels, Belgium
[b] Agilent Technologies Germany GmbH, Hewlett-Packard Str. 8, Waldbronn, BW 76337, Germany

ARTICLE INFO

Article history:
Received 5 November 2009
Received in revised form 5 January 2010
Accepted 22 January 2010
Available online 29 January 2010

Keywords:
Intermediate cooling
Ultra-high pressure
Temperature profiles
Column efficiency
Heat generation
Viscous friction
Adiabatic conditions
Isothermal conditions
Thermal environment

ABSTRACT

A generic solution is proposed for the deleterious viscous heating effects in adiabatic or near-adiabatic systems that can be expected when trying to push the column operating pressures above the currently available range of ultra-high pressures (i.e., 1200 bar). A set of proof-of-principle experiments, mainly using existing commercial equipment, is presented. The solution is based on splitting up a column with given length L into n segments with length L/n, and providing an active cooling to the capillaries connecting the segments. In this way, the viscous heat is removed at a location where the radial heat removal does not lead to an efficiency loss (i.e., in the thin connection capillaries), while the column segments can be operated under near-adiabatic conditions without suffering from an unacceptable rise of the mobile phase temperature. Experimental results indicate that the column segmentation does not lead to a significant efficiency loss (comparing the performance of a 10 cm column with a 2 cm × 5 cm column system), whereas, as expected, the system displays a much improved temperature stability, both in time (because of the shortened temperature transient times) and in space (reduction of the average axial temperature rise by a factor n). The method also prevents a large backflow of heat along the column wall that would lead to large efficiency losses if one would attempt to operate columns at pressures of 1500 bar or more. A real-world pharmaceutical example is given where this improved temperature robustness could help in moderating the changes in selectivity during method transfer from a low to a high pressure operation, although the complex non-linear behavior of the viscous heating and high pressure effects result in lower than expected improvement.

1. Introduction

The consequences of the presence of radial and axial temperature gradients inside chromatographic columns were recognized and discussed more than three decades ago [1,2] and were extensively studied on a theoretical and experimental basis by Poppe et al. [3,4]. The problem received a renewed attention in the recent years with the introduction of ultra-high pressure liquid chromatography (UHPLC) [5–10]. Theoretical, experimental and numerical studies all indicate that the thermal operating conditions strongly influence the performance of a chromatographic column. These thermal conditions vary between two limiting cases: adiabatic (no heat loss through the column wall) and isothermal (all heat is transported through the column wall which is kept at a fixed temperature). The increase of the mobile phase temperature $\Delta T_{\text{in-outlet}}$ (averaged over the column cross-section) between the inlet and the outlet of the column that can be expected in these cases is respectively given by [5,6,11,12]:

$$\text{Isothermal}: \quad \Delta T_{\text{inoutlet}} = (1 - \overline{\alpha \cdot T}) \cdot \frac{u_s \cdot (\Delta P/L) \cdot R^2}{8 \cdot \lambda_{\text{rad}}} \tag{1a}$$

$$\text{Adiabatic}: \quad \Delta T_{\text{inoutlet}} = (1 - \overline{\alpha \cdot T}) \cdot \frac{\Delta P}{C_{\text{p,V}}} \tag{1b}$$

where α is the coefficient of thermal expansion of the mobile phase, u_s the superficial velocity, ΔP the column pressure drop, L the column length, R the column's inner radius, λ_{rad} the radial thermal conductivity of the packed bed and $C_{\text{p,V}}$ is the volumetric heat capacity of the mobile phase and the horizontal dash denotes the column averaged value. For the typical organic solvents and operating pressures used in LC, it was shown that the so called "decompression heat" which is represented by the term $\alpha \cdot T$ (α defined as in Ref. [6]), and which counters the temperature increase, is of the order of 1/3 [6].

In the isothermal case ($T_w = T_{\text{in}}$), Eq. (1a) holds (in a first approximation [13]) along the entire length of the column ($\Delta T_{\text{bed,av}} = \Delta T_{\text{in-outlet}}$) for all distances extending beyond the thermal entrance length [3,13]. It should be noted that $\Delta T_{\text{in-outlet}}$ in

* Corresponding author. Tel.: +32 2 6293251; fax: +32 2 6293248.
E-mail address: gedesmet@vub.ac.be (G. Desmet).

0021-9673/$ – see front matter © 2010 Elsevier B.V. All rights reserved.
doi:10.1016/j.chroma.2010.01.072

the isothermal case is half that of the radial temperature gradient present in the column. In the adiabatic case, the average temperature increase (averaged over the length of the bed) equals half the ΔT-value given by Eq. (1b) ($\Delta T_{bed,av} = 0.5 \cdot \Delta T_{in-outlet}$) if a linear axial temperature gradient is assumed. The latter is a good approximation in a perfectly adiabatic and 'wall-less' case [14].

In general, the values of the temperature increase inside the column are around an order of magnitude larger in the adiabatic case than in the isothermal case:

$$\Delta T_{inoutlet,adiab} \gg \Delta T_{inoutlet,iso}, \quad (2)$$

and can easily top 20 °C for water if a column is operated near 1000 bar under close-to adiabatic conditions.

In terms of efficiency, there is also a distinct difference between the isothermal and the adiabatic case. In the former case, the presence of a radial gradient temperature leads to a strong additional contribution (H_{vh}) to the observed band broadening, whereas the pure axial T-gradient that is present in the idealized adiabatic case only leads to an insignificant effect on H:

Isothermal [11] :

$$H_{vh,iso} = \frac{1}{24} \cdot \frac{a^2}{2 \cdot (2+a)} \cdot u_{Rw} \cdot \frac{R^2}{D_{rad}} \quad \text{with } a = \frac{q \cdot R^2}{4 \cdot \lambda_{rad} \cdot T_{m,W}} \quad (3a)$$

Adiabatic :

$$H_{vh,adiab} \cong 0 \text{ (if backflow of heat along column wall and } P\text{- and } T\text{-effects on } D_{mol} \text{ and } k \text{ can be neglected)} \quad (3b)$$

where u_{Rw} is the retained species velocity and $T_{m,W}$ is the temperature of the mobile phase, both near the column wall, and D_{rad} is the solute's radial dispersion coefficient. Eq. (3a) shows that, under isothermal conditions, the viscous heat-induced additional plate height contribution depends very strongly on the column radius (up to a sixth-power dependency [11,15]. Eq. (3b) is no longer correct when P and T become so large that they have a significant effect on the molecular diffusion and retention coefficient of the analytes and can thus result in a measurable deviation of the normal plate height behavior. However, depending on the solvent and the interplay between pressure and temperature (who both have an opposite effect), this value can either be positive or negative, or can still remain insignificantly small (when the opposing effect cancel out each other) [9]. Eq. (3b) also no longer holds when the presence of the column wall is taken into account (see further on in the text). Anyhow, and despite the complexity of the latter effect, one can generally state that for normal-bore columns:

$$H_{vh,iso} \gg H_{vh,adiab} \quad (4)$$

In practice, a column is however seldom operated close to isothermal (i.e., thermostatted in a water or oil bath) or close to adiabatic (i.e., well insulated from the surrounding air), but is usually placed in a forced air- or a still air-oven. Because of the convection in the forced air-oven, a significant thermostatting effect is obtained, although air cooling is known to lead to heat transfer rates that are about an order or magnitude lower than when a cooling liquid is used [16]. The thermostatting effect is therefore generally not perfect in a forced air-oven. Applying 800 bar of total pressure, a temperature increase of about 5 °C has already been measured, see e.g., Fig. 2a in [17]. The natural convection occurring in the still air-oven case on the other hand leads to a heat transfer which is again around an order of magnitude lower than in the forced air case (air is a poor heat conductor). As a consequence, a still air-oven usually behaves closer to the adiabatic than to the isothermal case. Nevertheless, the measured temperature increases in a still air-oven are typically only about half that expected from Eq. (1a) [18], because the heat losses through the column wall remain significant.

Despite the above moderations, choosing between a still air- and a forced air-oven still roughly corresponds to choosing between the isothermal and adiabatic operation mode. Unfortunately, either way leads to an undesired drawback. In a still air-oven, the large ΔT_{in-out} of the near-adiabatic conditions can be expected to lead to a significant variation of the retention and diffusion properties of the solute along the column axis. In some rare cases, this temperature gradient can result in unexpected retention behavior such as a change in elution order of components or loss of selectivity when transferring methods to a higher pressure operation [19,20]. Operating a column in a well-thermostatted environment on the other hand results in more or less constant retention and diffusion properties along the column axis (except for the effects of pressure itself on the physiochemical properties [21]). However, the parabolic velocity profile that develops as a result of the thermostatting effect generally results in a very high loss of efficiency (cf. Eqs. (3a) and (4)). At ultra-high pressures (near 1000 bar), a loss of theoretical plates of more than 50% was reported by de Villiers et al. [5] when placing the column in a water bath and even an increase in reduced plate height by a factor 20 at the highest flow rate was reported by Gritti and Guiochon [22]. When operating the column in a forced air-oven, the loss in performance is smaller but still significant [17,23] and can even be observed at conventional HPLC pressures (400 bar) for 4.6 mm I.D. columns [10].

When using normal-bore columns (i.e., 2.1 mm or 4.6 mm I.D.) at ultra-high pressure, the loss in efficiency is in fact so large that still air-ovens clearly are to be preferred over forced air-ovens. However, the former type of thermal operation mode will also eventually reach a limit when trying to further increase the column pressures. It has namely already been reported that, when using high operating pressures (say 1000 bar and more), the H-values that are measured in still air-ovens are significantly larger than those theoretically expected [22,24,25]. This deviation is due to the presence of the column wall, which can, because of its high thermal mass, cause a significant back flow of heat from the end to the front of the column, in turn leading to the establishment of significant radial gradients (especially near the in- and outlet of the column), in turn causing a loss in efficiency [14,22,24–26]. Although the resulting radial flow profiles at the front and back of the column are inverse, these effects do not cancel each other out entirely [24,25]. Numerical simulations indicate that this problem will strongly aggravate when trying to push the operating pressures into the 1500–2000 bar range [24,25]. And even if one would succeed in solving the column wall backflow problem (for example by developing column containers with a sufficiently low axial heat conduction [14]), the axial temperature gradient that develops in the adiabatic case will eventually lead to a point wherein the retention capacity (and hence the separation) disappears near the end of the column [15]. Gritti and Guiochon calculated that the advantages of using very fine particles begin to disappear when more than 4 W/m of heat is dissipated in the packed bed [22].

Given the above, it is clear that one of the keys to a further increase of the operating pressure in LC [15] is to find a way to remove the generated viscous friction heat along the column axis without causing large radial temperature gradients inside the column. The former will result in more constant retention and selectivity properties, the latter in maintaining a high separation efficiency.

One obvious solution to solve the viscous heating problem would be to reduce the column diameter (using capillary columns instead of the standard 2.1 and 4.6 mm I.D. columns). However, there are many cases wherein the industry is still reluctant to reduce the column diameter (e.g., in pharmaceutical applications where the inevitably smaller detection sensitivity increases the risk

of missing some impurities). For these cases, the present paper investigates the possibilities of a generic solution to the viscous heating problem.

The principle behind the presently proposed solution is illustrated in Fig. 1 and consists of two parts. First, the column bed is split up into equal parts with a total length that corresponds to the original length and connecting them with thin connection capillaries (cf. the operation mode of coupled column systems [17,27–32]). Secondly, the connection capillaries are actively cooled to remove the generated heat in the preceding column segment. The advantage of removing the heat through the capillary wall instead of through the wall of the column, is the much smaller inner diameter of the former, so that the $H_{vh,iso}$-contribution remains insignificantly small (cf. the R^6-dependency in Eq. (3a)). The columns themselves can then be operated as closely as possible to the adiabatic case without risking to overheat the mobile phase, since it can be expected from the linear T-increase law given by Eq. (1b) that the axial temperature increase per segment will be n times smaller (if n is the number of column segments) than it would be in a non-split column with the same total length (as also the ΔP per column is n times smaller).

Following this approach it can be hoped to get the best from both worlds: the low temperature increase and stable temperature operation of an isothermal system, and the low loss in efficiency of an adiabatically operated system.

It should be noted that the solution proposed here is different form the solution investigated by for example Poppe and Welsch, who proposed to limit the effects of radial thermal gradients by introducing the mobile phase at a suitably chosen lower temperature than the oven temperature [4,22,33] so as to create adverse gradients to compensate for those resulting from viscous heating. It was reported that finding the optimal experimental conditions to minimize the efficiency loss might not be worth the trouble [15], since the undercooling will also depend on the mobile phase, flow rate and column dimensions used and hence changes for different separation conditions. In the present case, the produced heat is not countered by an a priori fixed change in mobile phase temperature, but is eliminated along the column axis. Doing so, actively controlled cooling systems can be used that can adapt their cooling rate to maintain a fixed set temperature, independently of the mobile phase composition or the flow rate.

The present paper reports on a proof-of-concept study investigating how well the proposed solution can be put into effect using the heat exchangers from a commercially available instrument, as well as by using more compact heat exchangers built in-house.

2. Experimental

2.1. Experimental conditions

Uracil (t_0-marker), butylparaben and methanol (MeOH) were purchased from Sigma–Aldrich (Steinheim, Germany). Acetonitrile (ACN) gradient grade for HPLC was purchased from Merck (Merck, Darmstadt, Germany) and HPLC grade water was prepared in the laboratory using a Milli-Q Advantage (Millipore, Bedford, MA, USA) water purification system. Methyl-4-(acetylamino)-2-hydroxybenzoate (P1), methyl-4-(acetylamino)-5-chloro-2-methoxybenzoate (P2) and methyl-4-(acetylamino)-5-chloro-2-methoxybenzoate (P3) were kindly provided by RIC (Kortrijk, Belgium). More information on the nature and structure of these compounds (P1–P3) is given in Ref. [19]. Waters Acquity UPLC BEH C18 2.1 mm × 50 mm, 2.1 mm × 100 mm and 2.1 mm × 150 mm (1.7 μm) columns were purchased from Waters (Milford, MA, USA). Samples consisting of 0.02 mg/ml uracil and 0.05 mg/ml propylparaben or 0.1 mg/ml of P1–P3 were dissolved in the initial mobile phase. The injected sample mixture volume was 1 μl for the propylparaben and 0.8 μl for the pharmaceutical compounds.

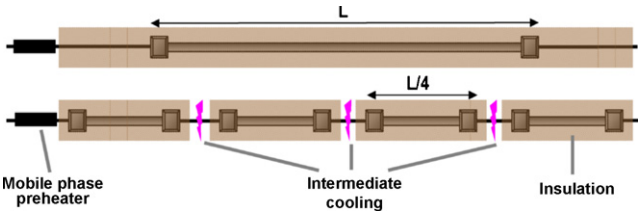

Fig. 1. Schematic representation of the principle of intermediate cooling for the removal of dissipated heat due to viscous heating without excessive loss of efficiency.

The measurements were performed on two different UHPLC systems. The first was a modified Agilent 1200 SL HPLC system (Agilent Technologies, Waldbronn, Germany) with a binary pump which could deliver a flow rate of 2 ml/min up till 1000 bar, a diode array detector with a Micro High Pressure flow cell, a modified injector to withstand the ultra-high pressure and a temperature controlled compartment with two additional commercial 1.6 μl low dispersion heat exchangers (Agilent Technologies, Waldbronn, Germany). The second was an Agilent 1290 Infinity system with a binary pump that can deliver a flow rate of 2 ml/min at 1200 bar. The system's maximum flow rate increases linearly with decreasing operating pressure to a maximum of 5 ml/min at 800 bar. The system also consisted of a diode array detector with a Max-Light cartridge cell (10 mm path length), an autosampler and a temperature controlled compartment with one additional 1.6 μl heat exchanger. Both systems were operated with Agilent Chemstation software.

The absorbance values were measured at 254 nm with a sample rate of 80 Hz for the butylparaben experiments and at 275 nm for the pharmaceutical compounds. The butylparaben measurements were performed in isocratic elution. The separation of the pharmaceutical sample was performed in gradient mode at a mobile phase inlet temperature of 37 °C, a mobile phase ramp from 5% to 57.5% ACN in H_2O with 0.25% ammonium acetate in a time t_G with $t_G/t_0 = 7.3$ and a delay time t_{del} with $t_{del}/t_0 = 0.24$, where both ratios were constant for the different flow rates [19].

2.2. Chromatographic system

Fig. 2a gives a schematic representation of the experimental setup with two coupled columns with intermediate cooling on the modified Agilent 1200 SL system. The mobile phase is first pumped through the 1.6 μl mobile phase heat exchanger (acting here as a phase pre-heater), then goes via the first column to enter a second mobile phase pre-heater, after which the flow continues to the second column and then finally reaches the detector. The setup for the single column experiments was similar, but only used one mobile phase pre-heater before the column. In Fig. 2b, the setup used on the Agilent 1290 Infinity system with three coupled columns is shown. In this case, the mobile phase passed again through a 1.6 μl pre-heater before entering the first column but continued to the two subsequent columns through 10 cm long, 120 μm inner diameter stainless steel capillaries, around which a home-made heat exchanger was constructed. For this purpose, a second (cooling) capillary with a larger inner diameter (250 μm) was coiled around each of the two connection capillaries over a distance of about 5 cm. The connection capillary and the cooling capillary were subsequently soldered together to achieve a minimal thermal resistance to heat transfer between the capillaries. A cooling liquid consisting of 90% water and 10% isopropanol was continuously recirculated from a solvent tank through the cooling capillary at 5 ml/min using an Agilent 1100 pump. To ensure an optimal heat transfer [34],

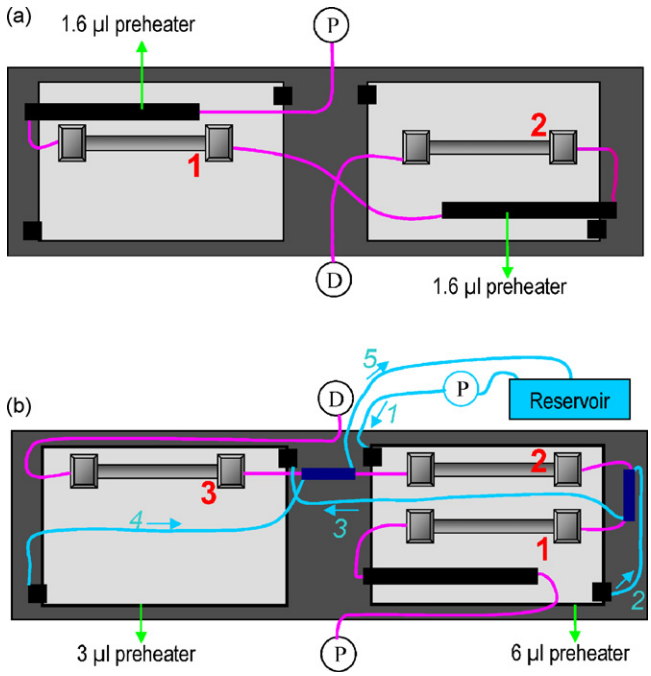

Fig. 2. (a) Experimental set-up to test the principle of intermediate cooling on the modified Agilent 1200 SL system (P = pump; D = detector). A 1.6 μl pre-heater was used for both preheating the mobile phase as for intermediate cooling. The pink lines represent the connecting capillaries for the mobile phase. (b) Experimental set-up to test the principle of intermediate cooling on the Agilent 1290 Infinity system. A second pump (Agilent 1100 system) was used to deliver a flow of 5 ml/min in the cool circuit (blue lines, 250 μm tubing) and the large mobile phase pre-heaters (left: 3 μl; right: 5 μl) to thermostat the mobile phase pumping through it. Arrows and italic numbers represent the flow direction. The dark blue rectangles represent the 5 cm of capillary around which the cooling capillary is cooled and soldered against it.

the cooling liquid was pumped in counter-current with the mobile phase flow flowing through the connection capillary. The temperature of the cooling liquid was controlled by passing it through the large (6 μl) and the small (3 μl) mobile phase pre-heaters in the temperature controlled compartment of the instrument. After the pump, the cooling liquid first passed through the 6 μl pre-heater (entrance and exit denoted by the black squares in Fig. 2), subsequently through the cooling capillary between the first and second column and the 3 μl pre-heater, and then via the cooling capillary between the second and third column back to the mobile phase reservoir. Despite the large length of the cooling circuit and the high flow rate, the pressure drop in the cooling circuit was below 100 bar, essentially because of the larger inner diameter of the tubing. Most of the pressure drop was in fact due to the mobile phase pre-heaters.

2.3. Temperature measurements

Temperature measurements were performed on the columns and connection capillaries using chromal–alumel thermocouples (J-type thermocouple wire) positioned as indicated in Figs. 3 and 4. To provide a perfect thermal contact, the two separate parts of the junction were point-welded directly onto the column or capillaries, using a device built in-house. The voltages were read out using a TBX-68T Isothermal Terminal Block (National Instruments, USA) and a NI 435X (National Instruments, USA) PCI card. The local temperature inside the thermal block was measured using a thermistor. In order to check the accuracy of the thermocouples, the read out was verified using an ice bath (0 °C), boiling water (100 °C) and a measurement at lab temperature (using a normal mercury thermometer as reference). The software used for the temperature read out was VI Logger (LabVIEW 6i, National Instruments). The measurement frequency was 1 Hz.

It should be noted here that the temperature measurements in the present study were mainly used as an indication of the column and mobile phase temperatures and for comparison between the different experimental cases. It is impossible to have exact values of the temperature inside the column bed and of the mobile phase in the connection capillaries without modifying the experimental setup and without disrupting the packing structure. Studies have been performed where the temperature of the eluent was directly measured and the temperature distribution inside the column was numerically determined [14,26], but such a detailed determination of the temperature profile is beyond the scope of this article.

3. Results and discussion

3.1. System design and heat removal capacity

To assess whether a short piece of thin connection capillary is sufficient to remove the heat that is being generated in the column segments, a classical expression found in many books on heat transfer [34], similar to that derived by Carr and co-workers [16,35,36], and valid for a fully developed laminar flow has been used (symbols explained in the symbol list):

$$\ln\left(\frac{T_w - T_{in}}{T_w - T_{out}}\right) = \frac{L_{cap}}{\rho \cdot F_V \cdot C_p} \cdot \left(\frac{1}{4.36 \cdot \pi \cdot \lambda_m} + \frac{\ln(R_{out}/R_{cap})}{2 \cdot \pi \cdot \lambda_w} + \frac{1}{2 \cdot \pi \cdot R_{out} \cdot h_{ext}}\right) \quad (5)$$

Eq. (5) shows that, if the heat transfer resistance in the tubing wall can be neglected compared to the two other mass transfer resistances (which is certainly the case when using metal connection tubing), the required tubing length is independent of the

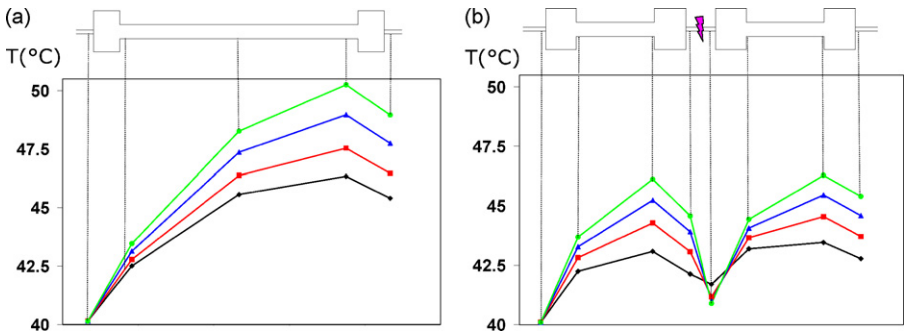

Fig. 3. Comparison of the experimentally measured temperatures of the column and capillary walls for the setup described in Fig. 2a, where the thermal behavior of one 10 cm long column (a) was compared with that of two coupled 5 cm columns (b) with intermediate active cooling for the flow rates (from top to bottom) of 0.49, 0.425, 0.35 and 0.24 ml/min of a 60/40% (v/v) MeOH/H_2O mixture at 40 °C in still air conditions.

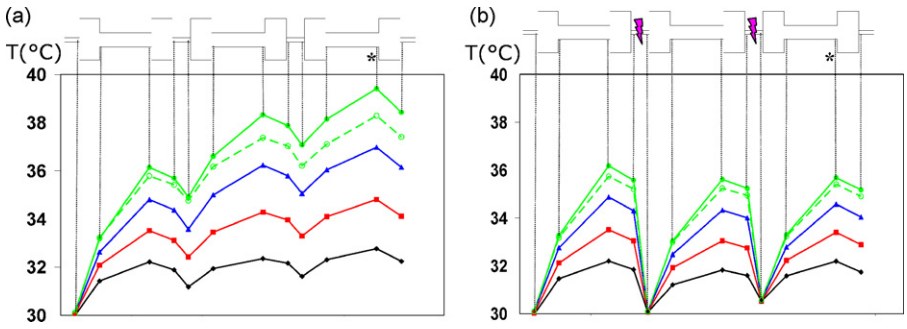

Fig. 4. Comparison of the experimentally measured temperatures of the column and capillary walls for the setup described in Fig. 2b, comparing a coupled system with three insulated columns, without (a) and with (b) active cooling applied, at flow rates of (top to bottom) 0.6, 0.5, 0.4 and 0.3 ml/min of a 45/55% (v/v) ACN/H_2O mixture at 30 °C. The dashed curve represents a measurement at 0.6 ml/min without column insulation. The connection capillaries and heat exchangers were not drawn to scale for sake of clarity.

inner tubing diameter [16]. In the present study, this has lead us to using tubing with an I.D. of 120 μm, as some kind of a compromise between the extra-column band broadening and the additional pressure drop of the connection capillaries.

Table 1a illustrates the length of tubing needed according to Eq. (5) to eliminate a given fraction of the temperature difference between incoming and outgoing liquid of the tubing in the isothermal wall case. The calculation was thus made for the best possible heat transfer conditions, obtained when the connection tubing is welded or soldered (very good thermal contact) onto a large heat sink that is well thermostatted to a fixed temperature (as was pursued during the experiments with the home-made heat exchangers shown in Figs. 2b and 4). In this case, the last two terms between the brackets in Eq. (5) are assumed to be small and the inner tubing temperature is assumed to be constant. In the latter case, the factor 4.36 (valid for a fixed wall heat flux) should be replaced by 3.66 [34]. The data in Table 1a then show that, for a flow rate of 2 ml/min pure water, it only takes 13.6 mm of tubing to reduce the difference between the incoming temperature (T_i) and a given set temperature (T_w) by half and 45.2 mm to reduce it to 10%. As already mentioned, this distance is independent of the tubing inner diameter and also increases linearly with the mobile phase flow rate (or equivalently with the mass flow $\rho \cdot F_V = \dot{m}$). In practice the necessary tubing will be larger since the tubing wall will never be perfectly isothermal. If e.g., a water or oil bath would be used to cool the capillary instead of a soldered heat sink, the total heat transfer resistance will be more or less twice as large [16] and hence will also be the necessary tubing length. However, if the needed tubing length would turn out to be too large (for example if a flow rate of 5 ml/min or more should be treated), the sink temperature can be set slightly (1 or 2 °C) below the desired outlet temperature. This allows a significant reduction of the necessary tubing length, as is illustrated in Table 1b. The strong effect of this slight undercooling can be explained by the exponential decrease of the temperature difference variation with tubing length, making it very hard to remove the last temperature bias between wall and mobile phase.

The above derivations and calculations also show that it should be possible to use one of the 1.6 μl mobile phase pre-heaters of the commercial instrument we employed as the intermediate cooling unit, because this type of heat exchanger has a tubing length of more than 100 mm and is in contact with a large thermal mass at a fixed temperature. The downside of using this pre-heater for the intermediate cooling is the large extra-column volume it introduced, since there is also tubing needed to connect it with the two columns. Therefore, a more compact heat exchanger set-up was constructed as well. With this system, consisting of a cooling capillary directly soldered onto the connection capillary (see Section 2), a temperature difference of 15 °C could be eliminated at a flow rate of 1.2 ml/min.

3.2. Achieved intermediate cooling performance

Fig. 3 compares the temperature increase along a 10 cm long column (left) and two coupled 5 cm columns (right) with intermediate active cooling. The columns were placed in the temperature controlled compartment (i.e., a still air-oven) of the instrument. As can clearly be seen, the temperature increase on the coupled column system with active cooling has an amplitude that is slightly above one half of that in the longer column ($\Delta T_{in-outlet}$ = 6.2 °C vs. 10.3 °C at the highest flow rate respectively). The fact that the measured $\Delta T_{in-outlet}$ is slightly larger than can be expected from the linear T-increase law given by Eq. (1b) and leading to an expected value of $\Delta T_{in-outlet} = \Delta T_{single}/2 = 5.15°$, is in part is due to the fact that the temperature of the mobile phase at the end of the heat exchanger did not decrease to the set temperature of the oven. Measurements of the temperature across the temperature controlled compartment showed that the latter was not due to an insufficient cooling capacity, but was due to an uneven temperature distribution in the oven, resulting in a deviation from the set temperature in both the heat exchangers and the air around the connecting capillaries.

Another factor explaining why the observed temperature increase is not exactly equal to $\Delta T_{single}/n$ is to be found in the fact that the T-profile along the single column is not linear but displays

Table 1a
Necessary tubing length to decrease or increase the difference of the mobile phase temperature to the set temperature for different flow rates calculated using Eq. (5). The following properties (i.e., those of water at 30 °C) were chosen for the mobile phase: λ_m = 0.615 W/m K, C_p = 4178 J/kg K, ρ = 996 kg/m^3) and fully developed, laminar flow in a capillary with a fixed wall temperature was assumed.

$(T_w - T_{in})/(T_w - T_{out})$ (%)	L (mm)	
	F = 1 ml/min	F = 2 ml/min
50	6.8	13.6
75	13.6	27.2
90	22.6	45.2
99	45.2	90.3

Table 1b
Necessary tubing length needed to decrease the mobile phase temperature from 40 °C (T_{in}) to a given temperature (T_{out}) using a heat sink (isothermal tubing wall) set at different temperatures (T_w). The flow rate was set to 2 ml/min and the same conditions as in Table 1a are used.

T_{out} (°C)	L (mm)		
	T_w = 30 °C	T_w = 29 °C	T_w = 28 °C
35	13.6	11.9	10.6
32.5	27.2	22.5	19.2
31	45.2	33.4	27.2
30.1	90.3	45.2	34.2

a convex downward curvature. This downward curvature has three causes: firstly, the temperature bias between the column and the oven compartment is larger in the second part of the column than in the first part of the column. As a consequence, a larger fraction of the generated heat is being lost to the environment in this second part. Secondly, the viscosity in the second part of the column is also lower than in the first part so that also less heat is being generated there. Thirdly, the backflow of heat through the column wall also leads to a flattening of the axial temperature profile on the wall. In the coupled column system, the temperature in each segment never rises above that in the first part of the single column system, so that the temperature increase in each individual segment will rather resemble that of the first part of the single column, hence explaining why the measured ΔT is larger than the $\Delta T_{single}/n$-value expected from the linear T-increase law. This deviation is also confirmed in the three-segment systems studied in Fig. 4 further on and is partly a consequence of the fact that we could not use the columns in a perfectly adiabatic mode, resulting in the loss of some of the generated heat through the outer column walls. Although this might appear to be advantageous to limit the temperature increase of the mobile phase, it should be recalled here that the removal of heat through the column wall introduces radial temperature and velocity gradients in the column, which are best avoided to maintain high efficiency, as was demonstrated in the introduction.

Fig. 4 compares the temperature evolution in two three-segment systems (3 cm × 5 cm), one without (Fig. 4a) and one with active cooling (Fig. 4b). In this setup, the columns as well as the connection capillaries were all insulated (using commercial tubing insulation) from the surrounding air and placed in the temperature controlled compartment of the instrument. The insulation however did not result in a perfectly adiabatic system as can be seen in Fig. 4, where the dashed curve shows the measured temperature profile at the highest flow rate when none of the columns or connection capillaries were insulated but were simply placed in the temperature controlled compartment. Although this leads to a smaller temperature increase (ΔT = 5.7 °C vs. 6.2 °C at the highest flow rate at the end of the first column) than the insulated column case, the latter clearly behaves far from adiabatic, as this operation mode should normally lead to a much larger temperature difference (50–100% larger ΔT). One of the main reasons for this deviation, besides the finite thermal resistance of the insulation material, is the fact that adding insulation to the column also increases its outer surface and therefore the area over which it dissipates heat to the environment. A similar effect can also be seen in Fig. 4a, where the temperature in the connection capillaries also slightly decreases (around 1 °C for the highest flow rates), despite that they are also insulated.

Similar to what was observed in the two-segment system in Fig. 3, we here again note that the temperature increase is larger than the expected $\Delta T_{single}/n$-value. Comparing the temperature increase of a single 15 cm long column (data: see bottom curve in Fig. 8a) with the actively cooled system, it is observed that the average temperature increase is not a factor 3 lower as expected, but only a factor of around 2.5. As already explained when discussing Fig. 3, the reason for the higher than expected temperature increase is not due a poor heat removal in the intermediate heat exchangers, but to the fact that the more downstream parts of the single column heat up less than the first parts, while the individual segments rather behave as the first part of the single column (first 1/nth-part in case of n segments). In the present case, the experimental observations were further affected by the fact that the 5 cm columns had a 20% lower permeability than the 15 cm column. The higher pressure drop results in a larger amount of heat generated in the column, which in turn certainly also contributed to a higher than expected heating in the three-segment system compared to the single 15 cm column.

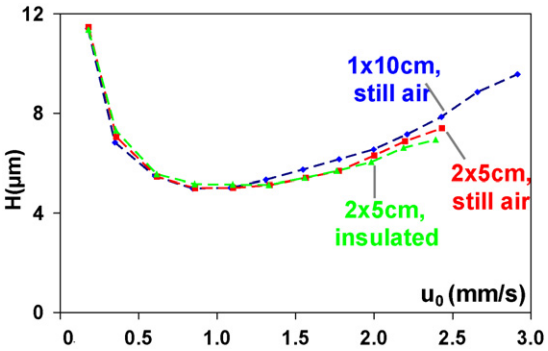

Fig. 5. Comparison of the isocratic column performance on a single 10 cm column (♦) and two coupled 5 cm columns with intermediate cooling (■) in still air conditions and 2 cm × 5 cm in adiabatic conditions (▲). The test component was propylparaben (k' = 5.4) and the mobile phase composition 60/40% (v/v) MeOH/H_2O at a temperature of 25 °C.

In the active cooling case, the temperature after the first and second column returns almost perfectly to that of the incoming liquid in the first column (coming from the mobile phase pre-heater) and thus to that of the temperature controlled compartment. The small T-difference remains for the heat exchanger between columns 2 and 3, but this is again most probably due to a small variation in oven temperature, resulting in a higher temperature for the cooling liquid exiting the second (3 μl) heat exchanger. If the effect would have resulted from a poorly designed heat exchanger (e.g., too short), it would become more pronounced with higher flow rates, which is clearly not the case in Fig. 4b. The temperature profile Fig. 4b shows that the temperature distribution in each of the segments of the 15 cm length column system (operated e.g., 990 bar) is more or less identical to that in a single 5 cm long column operated at this flow rate (at an equivalent pressure drop of 330 bar). This approach, wherein a column is split up into different segments that all operate under the low viscous heating conditions of a sub-400 bar system, can in principle be applied *ad infinitum*. Even pressures way beyond those currently used are conceivable. For example, splitting up a column operated at 4000 bar into 10 different segments, would lead to a situation wherein each column segment thermally behaves as if it were only operated at a pressure of 400 bar.

The case without active cooling (Fig. 4a) also shows that the rate of the temperature increase gradually decreases with increasing distance in the coupled column system. This is due to the lower heat generation in the more downstream parts of the column system, since the viscosity decreases more with increasing mobile phase temperature than the volumetric flow rate increases, and, as already mentioned, because of the larger heat loss to the environment as a result of the larger temperature bias with the surroundings. An additional effect that contributes to the convex downward curvature of the temperature profile along a single column is the backflow of heat from the column exit to the front of the column [12,24–26,37].

3.3. Effect on efficiency

Fig. 5 compares the performance of a single column with that of two different coupled column systems with intermediate active cooling. As can be seen, all systems display a nearly identical efficiency for the lower flow rates (B-term range and region around the optimal velocity u_{opt}). In the high flow rate regime, the coupled column systems exhibit a slightly better performance than the single column system. Although it is difficult to draw any hard general conclusions from this experiment (the difference between the 10 cm and the 2 cm × 5 cm columns might also be

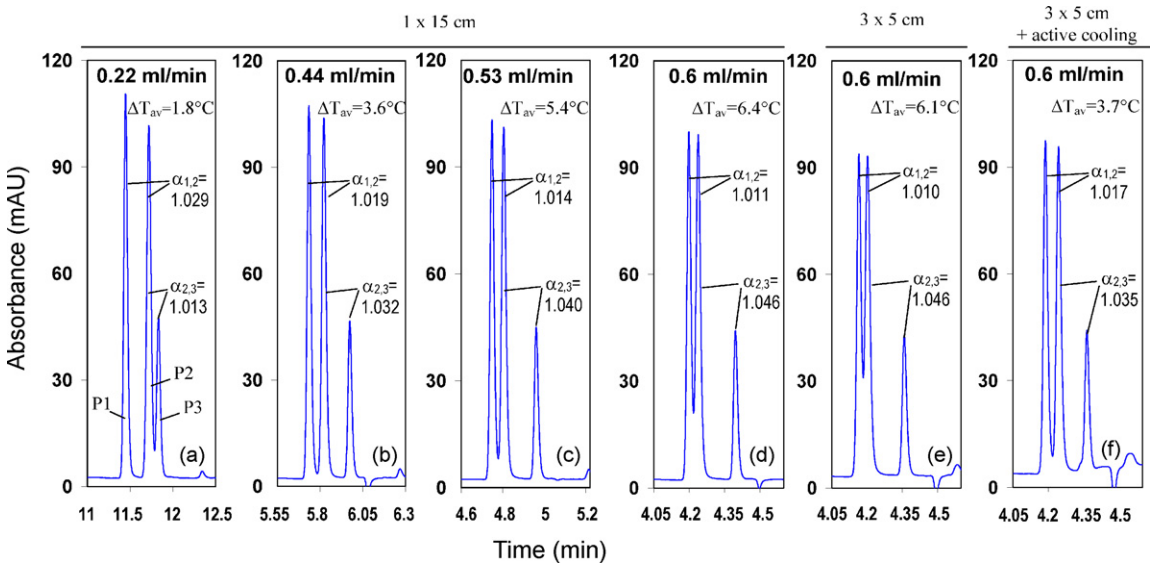

Fig. 6. Comparison of the recorded chromatograms of three impurities in metoclopramide hydro-chloride formulations using a gradient separation as described in Section 2.1. (a)–(d) represent the observed results on a 15 cm long column with increasing flow rate, (d) shows at the chromatogram at the same flow rate but for a coupled system without active cooling and (e) represent the same experiment but now with the active cooling on.

due to differences in packing quality between the long and the short columns), the least we can conclude is that the segmentation of a 10 cm column into two 5 cm segments does not lead to an unallowable loss in efficiency. Noting that the thermal conditions have a clear effect on the two coupled column cases (the segmented system wherein the columns are thermally insulated has a slightly better performance than that wherein the columns are not insulated), the slightly better performance of the two coupled column systems compared to the single column system would be in agreement with the smaller temperature differences between the column and the environment. This smaller temperature difference reduces the radial velocity gradients inside the column, which in turn can be expected to result in a slightly higher performance in the higher flow rate regime. It was however not possible to reach the same high flow rates with the coupled columns as with the single column system, partly because of the additional pressure drop in the connection capillary (although this only amounts up to some 12 bar at a flow rate of 1 ml/min for a 50/50%, v/v, MeOH–H_2O mixture), but especially due to the lower temperature increase in the coupled column system, which in turn leads to a higher mobile phase viscosity (when it comes to pressure drop, increases in temperature have an advantage).

3.4. Effect on selectivity

Fig. 6 compares the chromatograms recorded in gradient elution of the three pharmaceutical compounds (P1–3) described in Section 2.1 on a 15 cm long column at different flow rates (Fig. 6a–d), reflecting the sequence of separations one would go through if trying to speed up the separation method on a given column by raising the pressure from the reference case (400 bar, 0.22 ml/min) to the ultra-high pressure range. As can be clearly observed, the selectivity between the different components shifts considerably for an increase in flow rate and hence operating pressure. As was shown by Sandra and co-workers [19,20], this is clearly a result of the higher average column temperature due to viscous heating since this effect could in part be remedied by lowering the oven and mobile phase inlet temperature. The effect of temperature on retention is clearly higher for P2 than for P1 and P3. As a consequence, the selectivity of the triplet drastically changes compared to that of the original separation (Fig. 6a). The same selectivity shifts are noted for the system with three coupled 5 cm columns going from 0.22 ml/min up till 0.6 ml/min without active cooling applied (only the results at the highest flow rate are shown, see Fig. 6e), although this system already exhibits a slightly lower temperature increase due to the inherent cooling effect of the connection capillaries (the full set of chromatograms for the coupled column system can be found in the Supporting Material, SM). There is a small difference in selectivity shift between the 15 cm column and 3 cm × 5 cm column, resulting in a $\Delta\alpha_{1,2}$ of 0.018 for the 15 cm column and 0.017 for the 3 cm × 5 cm columns when going from a flow rate of 0.22–0.6 ml/min.

Fig. 6f shows the same system as in Fig. 6e but now with the active cooling switched on (see the SM for the chromatograms at lower flow rates). Where the cooled coupled system at 0.22 ml/min exhibits a similar selectivity as on the 15 cm column, it can be clearly observed that the selectivity shift going to 0.6 ml/min is significantly smaller (only 0.008) than that on the 15 cm column or in the 3 cm × 5 cm system without active cooling. However, based on the fact that the column was split up in three parts, theoretically a similar selectivity as that at 0.22 ml/min (e.g., as Fig. 6a) could have been expected. The fact that this did not occur is a combination of different factors. As mentioned in Section 3.2, the temperature increase in the coupled system is larger than expected. The average column temperatures given in Fig. 6 (calculated by taking the average of all measured temperature values on the column walls) clearly illustrates this effect. The $\Delta T_{av} = 3.7\,^{\circ}C$ that was measured on the actively cooled system is significantly larger than the $\Delta T_{av} = \Delta T_{single}/n = 6.4/3 = 2.1\,^{\circ}C$ that would be expected from the linear T-increase law. In addition, the 3 cm × 5 cm columns exhibited a slightly different selectivity than the 15 cm long column ($\alpha_{1,2} = 1.010$ vs. 1.011) and it is also not impossible that a part of the observed selectivity change is pressure induced [21].

Despite this deviation, the intermediate cooling improves the selectivity at the highest flow rate compared to the single column. In fact, the shift in selectivity ($\Delta\alpha_{1,2} = 0.008$) is of the same order as that obtained in the single column system for a flow rate of 0.44 ml/min ($\Delta\alpha_{1,2} = 0.010$), in agreement with the fact that the average temperature rise at this flow rate is about the same as in the coupled column system.

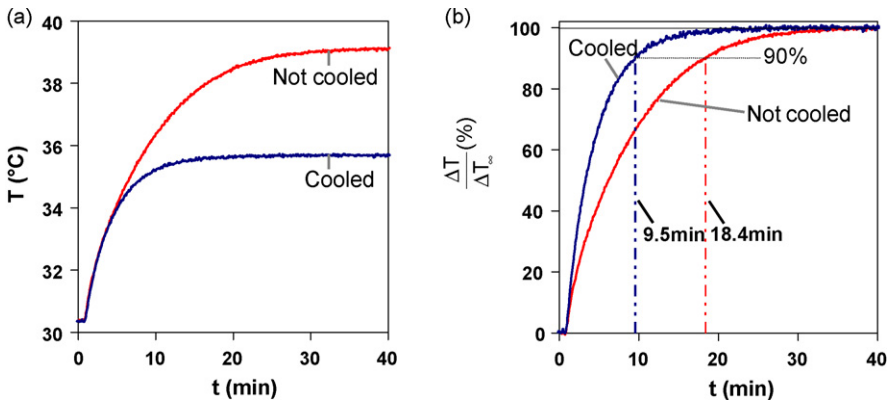

Fig. 7. (a) Thermal response of a coupled column system without (red curve) and with (blue curve) active cooling when switching the flow rate from 0.15 to 0.6 ml/min 45/55% (v/v) ACN/H_2O mixture at 30 °C. The data relate to the temperature read out from the end of the last column (denoted by the "*" in Fig. 4). (b) Same data as (a) but now the temperature variation is plotted relative to its long time limit (i.e., steady state) value. (For interpretation of the references to color in this figure legend, the reader is referred to the web version of the article.)

3.5. Effect on temperature equilibration times

Whereas the above observations relate to steady-state operations, it should not be forgotten that each change in flow rate or mobile phase composition that is made on an instrument leads to a transient regime wherein the temperature transits from one to another steady-state temperature [15]. It goes without saying that the instrument's temperature robustness improves when this transient regime can be kept as short as possible. Fig. 7a shows the thermal response of the coupled columns system shown in Fig. 4 by plotting the measured temperature of the final thermocouple attached to the end of the third column (denoted by a "*" in Fig. 4) as a function of time when the flow rate was switched from 0.15 ml/min (ΔP_∞ = 313 bar) to 0.6 ml/min (ΔP_∞ = 1080 bar). The column was in thermal steady state at the start of the measurement (F_V = 0.15 ml/min) and the evolution of the temperature was followed till this steady state was reached for the higher flow rate. As expected and also visible from Fig. 4, the cooled coupled column system reaches a steady-state temperature which is lower than in the uncooled system. However, more importantly, the thermal steady state is reached almost twice as fast for the cooled coupled system, than for the uncooled, as is shown in Fig. 7b, where the relative temperature increase (vs. its steady-state values) is plotted as a function of time. The faster thermal response and lower temperature increase will also give advantages for gradient elution. In this case, the pressure drop over a column varies during a gradient run since the mobile phase composition and hence the average viscosity varies over time [38]. This also results in a variation of the generated heat and therefore also of the average column temperature.

3.6. An outlook on the use of higher pressures

In Fig. 8, an attempt is made to assess the advantage of intermediate cooling if one would want to use higher operating pressure than those currently available in commercial systems. In Fig. 8a, the experimentally measured temperature increase along a 15 cm long column (insulated) at 1080 bar is plotted (bottom curve), along with the extrapolated expected temperature increase at 1500 and 2000 bar. The extrapolation was performed in the following manner: the temperature increase on a given location increased almost perfectly linearly with the mobile phase rate ($R^2 > 0.999$), while the pressure increase with the mobile phase velocity was fitted with a second order polynomial. Theoretically, if the viscosity would be independent of pressure and if no heating would occur, the pressure drop over the column would increase linearly with the flow rate. In practice, the viscosity increases with increasing pressure, but also decreases with the increase in mobile phase temperature due to viscous heating. Since the latter effect is stronger than the former in near-adiabatic operation, the pressure flow rate curve exhibits a slight downward curvature that cannot be expressed with a linear fit. Using a polynomial function (second order) to fit this trend, the necessary flow rate to reach 1500 or 2000 bar pressure drop was calculated and this flow rate was subsequently used in the linear fit of (F_V, ΔT) to calculate the expected temperature increase. Although this is a crude extrapolation, it still gives a good indication of the temperature increases expected at operation of columns at these pressures.

Fig. 8b shows that simply coupling the columns without active cooling already reduces the total temperature increase (because of the efficient cooling under natural convection conditions occurring in the connection capillaries), although nearly not as much as the active cooling system shown in Fig. 8c. In addition, this type of natural cooling is not controlled so that the column temperature would still fluctuate depending on the mobile phase composition and the flow rate. Fig. 8c shows that the temperature increase on the coupled system with active intermediate cooling can be expected to reduce the total average temperature increase by half compared to the single column system shown in Fig. 8a. Of course, using even more column segments with intermediate cooling would result in an even more constant temperature along the column bed.

As the latter in principle opens the road to an unprecedented range of operating pressures (at least for what concerns the viscous heating problem), it should also be considered that the produced viscous friction heat is also partly advantageous for some aspects of the separation (viscosity, diffusion coefficient, retention shift). This is due to the fact that an increased temperature generally counters the pure effect of the pressure on the physico-chemical properties of the mobile phases and the solutes, causing shifts in retention and decrease of diffusion coefficients. To get the best of both worlds (temperature robustness and suppression of high pressure effects on diffusion rates and shifts in selectivity), the presently proposed method could be applied in a segmented oven, wherein each compartment is used at a different temperature to compensate for the nefarious effects of pressures. Since the effect of temperature on viscosity, diffusions coefficients and retention is in general in the opposite sense of that of pressure, operating the first columns at a slightly higher temperature than the subsequent ones could compensate for the negative effect of the pressure alone. This could e.g., be realized for a four column system operated at 4000 bar where the first column is operated at a temperature of 45 °C and a

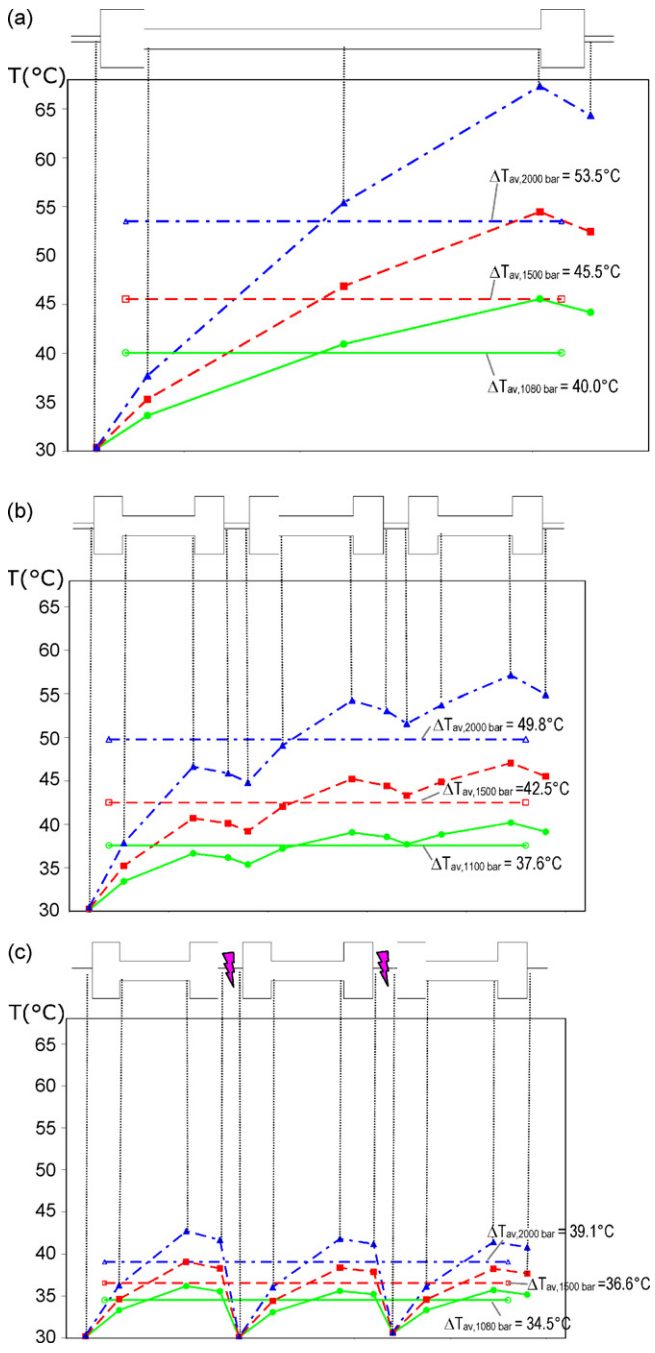

Fig. 8. Extrapolation, as described in Section 3.6, of the measured temperature profiles at 1080 bar (●) operating pressure to 1500 bar (■) and 2000 bar (▲) on a (a) 15 cm long column, (b) 3 cm × 5 cm long column without active cooling and (c) 3 cm × 5 cm long column with active cooling. Same experimental conditions as described for Fig. 4.

pressure between 4000 and 3000 bar, the second at 40 °C between 3000 and 2000 bar and the third and fourth at 35 °C and 30 °C respectively.

4. Conclusions

The use of a coupled column system with active cooling applied to the intermediate connection capillaries is shown to be a promising solution for the removal of the generated heat by viscous friction in liquid chromatography columns. By limiting the pressure drop per column segment to those commonly occurring in HPLC (i.e., around 400 bar), the effects of the use of ultra-high pressure can be limited to the extent of those observed in normal HPLC operation.

To be more precise, the concept of splitting up a column into n different segments with active intermediate cooling approximately allows to limit the total increase of the mobile phase temperature to that occurring in the first 1/*n*th-part of the single column reference system. In the present study, this was exemplified by showing that the observed temperatures increase along a column bed can be decreased by a factor of 2 by splitting up the column in two or three separate parts. Keeping the individual segments 5 cm or larger, the column segmentation can be realized without significant loss in performance. In the present study, even a slightly higher performance was observed in the high flow rate region of the van Deemter curve, i.e., the region that is most prone to viscous heating effects.

The principle of intermediate cooling can also be advantageous to transfer separation methods from low to high pressure operations if the sample contains analytes with a different retention dependency on the temperature. As was demonstrated for a real-world pharmaceutical example, the improved temperature robustness allows to more closely maintain the low pressure selectivity of the separation when switching to a faster method at higher pressures, although the non-linearity of the viscous heating effects resulted in a smaller improvement than expected.

The intermediate cooling technique also leads to a faster thermal equilibration of the column system, resulting in more reproducible results of separations and faster thermal re-equilibration of the columns after e.g., gradient runs or changes in flow rate.

Further study is however needed to make more detailed assessments of the effect of the additional extra-column volume, column endfittings and frits of the coupled column system versus a single column, although theses results will always be obscured by the inevitable column-to-column variability of the performance, the permeability and the retention and by the fact that longer columns frequently lead to higher plate height values than shorter ones as longer columns apparently are more difficult to pack [15]. In addition, it must be investigated how small the intermediate cooling system can be made from an engineering point of view. Theoretically, data in Table 1b show that applying a small degree of undercooling to the capillary wall results in the need of only very short capillaries for thermostatting the mobile phase.

Although the gain observed in the current work might still be limited, the ongoing pursuit of ever higher operating pressures in commercial instruments will soon require adjustments, such as those presented in the current work, to maintain column efficiency and selectivity. It is believed that the presented solution will remove the upper limit on operating pressures in liquid chromatography systems from a viscous heating point of view. There are however numerous other problems (e.g., mechanical stability of columns, pumps, valves, injectors, particles, etc.) that need to be solved by instrument and column manufacturers before systems operated at pressures of 2000 bar and beyond can be commercially available (reproducible, durable and affordable).

Nomenclature

C_p	specific heat capacity of the mobile phase (J/kg K)
$C_{p,V}$	volumetric mobile phase heat capacity (J/m^3 K)
D_{rad}	radial dispersion coefficient (m^2/s)
F_V	volumetric flow rate (m^3/s)
h_{ext}	heat transfer coefficient at the outer surface of a capillary (W/m K)
L	column length (m)
L_{cap}	tubing/capillary length (m)
Nu	Nusselt number
q	volumetric heat generation (W/m^3)

R column inner radius (m)
R_{cap} tubing/capillary inner radius (m)
R_{out} tubing/capillary outer radius (m)
$T_{m,W}$ temperature of mobile phase near the column wall [11] (K)
T_w, T_{in}, T_{out} temperatures of the capillary wall (cooling temperature), incoming liquid and exiting liquid of the capillary (K)
ΔT temperature difference (K)
ΔP column pressure drop (Pa)
u_{Rw} retained species velocity near the column wall [11] (m/s)
u_s superficial velocity, i.e., F_V divided by the column cross-section (m/s)

Greek symbols
α mobile phase coefficient of thermal expansion (1/K)
$\alpha_{i,j}$ selectivity between components i and j, defined as $\alpha_{i,j} = k_j/k_i$
λ_{rad} radial thermal conductivity of the packed bed (W/m K)
λ_m mobile phase thermal conductivity (W/m K)
ρ mobile phase density (kg/m^3)

Subscripts
adiab adiabatic (no heat loss) operation
av averaged
bed column bed, i.e., both particles and mobile phase
in incoming
in–outlet difference between incoming and exiting mobile phase in column
iso isothermal (fixed wall temperature) operation
out outgoing
vh viscous heating
w wall
∞ long time limit, i.e., after thermal equilibration

Acknowledgements

The Department of Chemical Engineering of the VUB gratefully acknowledges the loan of a modified Agilent 1200 SL system from Agilent Waldbronn GmbH and an "Agilent Technologies Award for Excellence in Collaborative Research" from the Agilent Technologies Foundation. K.B., J.B. and M.V. all gratefully acknowledge research grants from the Research Foundation – Flanders (FWO Vlaanderen). Prof. P. Sandra and Dr. G. Vanhoenacker (Kortrijk, Belgium) are kindly thanked for providing the pharmaceutical compounds.

Appendix A. Supplementary data

Supplementary data associated with this article can be found, in the online version, at doi:10.1016/j.chroma.2010.01.072.

References

[1] I. Halász, R. Endele, J. Asshauer, J. Chromatogr. 112 (1975) 37.
[2] Cs. Horvath, H.-J. Lin, J. Chromatogr. 149 (1978) 43.
[3] H. Poppe, J.C. Kraak, J.F.K. Huber, J.H.M. Van den Berg, Chromatographia 14 (1981) 515.
[4] H. Poppe, J.C. Kraak, J. Chromatogr. 282 (1983) 399.
[5] A. de Villiers, H. Lauer, R. Szucs, S. Goodall, P. Sandra, J. Chromatogr. A 1113 (2009) 84.
[6] M. Martin, G. Guiochon, J. Chromatogr. A 1090 (2005) 16.
[7] F. Gritti, G. Guiochon, J. Chromatogr. A 1131 (2006) 151.
[8] F. Gritti, G. Guiochon, J. Chromatogr. A 1138 (2007) 141.
[9] U.D. Neue, M. Kele, J. Chromatogr. A 1149 (2007) 236.
[10] M.M. Fallas, M.R. Hadley, D.V. McCalley, J. Chromatogr. A 1216 (2009) 3961.
[11] G. Desmet, J. Chromatogr. A 1116 (2006) 89–96.
[12] F. Gritti, G. Guiochon, Anal. Chem. 81 (2009) 3365.
[13] K. Kaczmarski, J. Kostka, W. Zapała, G. Guiochon, J. Chromatogr. A 1216 (2009) 6560.
[14] K. Kaczmarski, F. Gritti, J. Kostka, G. Guiochon, J. Chromatogr. A 1216 (2009) 6575.
[15] G. Guiochon, J. Chromatogr. A 1126 (2006) 6.
[16] J.D. Thompson, J.S. Brown, P.W. Carr, Anal. Chem. 73 (2001) 3340.
[17] D. Cabooter, F. Lestremau, A. de Villiers, K. Broeckhoven, F. Lynen, P. Sandra, G. Desmet, J. Chromatogr. A 1216 (2009) 3895.
[18] F. Gritti, G. Guiochon, Anal. Chem. 80 (2008) 6488.
[19] G. Vanhoenacker, F. David, B. Blatz, E. Naegele, P. Sandra, Increasing Productivity in the Analysis of Impurities in Metoclopramide Hydro-chloride Formulations Using the Agilent 1290 Infinity LC System, 2009. http://cp.chem.agilent.com/Library/applications/5990-3981EN.pdf.
[20] P. Sandra, R. Szucs, M. Hanna-Brown, Presented at the 33rd International Symposium on High Performance Liquid Phase Separations and Related Techniques (HPLC 2009), Dresden, Germany, 28 June–2 July, 2007 (Plenary Lecture 01).
[21] M.M. Fallas, U.D. Neue, M.R. Hadley, D.V. McCalley, J. Chromatogr. A 1209 (2008) 195.
[22] F. Gritti, G. Guiochon, J. Chromatogr. A 1216 (2009) 1353.
[23] K. Broeckhoven, J. Billen, M. Verstraeten, K. Choikhet, M. Dittmann, G. Rozing, G. Desmet, Presented at the 8th Balaton Symposium on High-performance Separation Methods, Siófok, Hungary, September 2–4, 2009 (Lecture-38).
[24] K. Broeckhoven, J. Billen, G. Desmet, K. Choikhet, G. Rozing, Presented at the 31st International Symposium on High Performance Liquid Phase Separations and Related Techniques (HPLC 2007), Ghent, June 17–21, 2007 (Lecture L22.01).
[25] K. Broeckhoven, K. Choikhet, G. Rozing, G. Desmet, Poster Presented at the 32nd International Symposium on High Performance Liquid Phase Separations and Related Techniques, Baltimore, MD, USA, May 10–16, 2008 (P03.25).
[26] F. Gritti, G. Guiochon, Anal. Chem. 80 (2008) 5009.
[27] F. Lestremau, A. de Villiers, F. Lynen, A. Cooper, R. Szucs, P. Sandra, J. Chromatogr. A 1138 (2007) 120.
[28] F. Lestremau, A. Cooper, R. Szucs, F. David, P. Sandra, J. Chromatogr. A 1109 (2006) 191.
[29] D.V. McCalley, J. Chromatogr. A 1193 (2008) 85.
[30] J.M. Cunliffe, T.D. Maloney, J. Sep. Sci. 30 (2007) 3104.
[31] D. Cabooter, F. Lestremau, F. Lynen, P. Sandra, G. Desmet, J. Chromatogr. A 1212 (2008) 23.
[32] D.V. McCalley, R.G. Brereton, J. Chromatogr. A 828 (1998) 407.
[33] T. Welsch, M. Schmid, J. Kutter, A. Kálman, J. Chromatogr. A 728 (1996) 299.
[34] Y.A. Çengel, Heat Transfer—A Practical Approach, 2nd ed., McGraw Hill, New York, 2003 (Chapter 8).
[35] B. Yang, J. Zhao, J.S. Brown, J. Blackwell, P.W. Carr, Anal. Chem. 72 (2000) 1253.
[36] D. Guillarme, S. Heinisch, J.-L. Rocca, J. Chromatogr. A 1052 (2004) 39.
[37] K. Kaczmarski, F. Gritti, G. Guiochon, J. Chromatogr. A 1177 (2008) 92.
[38] K. Broeckhoven, K. Choikhet, M. Dittmann, G. Rozing, G. Desmet, Poster Presented at the 33rd International Symposium on High Performance Liquid Phase Separations and Related Techniques (HPLC 2009), Dresden, Germany, June 28–July 2, 2009 (Poster ALM05).